Journal of Renewable Materials

Tech Science Press

DOI: 10.32604/jrm.2023.022535

ARTICLE

Synthesis and Antioxidant Activity of (E) ω-Formylcamphene-Based Thiazole Hydrazone Derivatives

Jiayu Chang[1], Qingying Ding[1], Chong Zhong[1], Yao Long[2], Zhuanquan Xiao[3], Hai Luo[1], Yuling Yang[1], Zongde Wang[1], Shengliang Liao[1], Jinzhu Chen[2], Shangxing Chen[1,*] and Ji Zhang[1,*]

[1]College of Forestry, Jiangxi Agricultural University, East China Woody Fragrance and Flavor Engineering Research Center of National Forestry and Grassland Administration, Camphor Engineering Research Center of NFGA, Nanchang, 330045, China

[2]College of Science, Jiangxi Agricultural University, Nanchang, 330045, China

[3]College of Chemistry and Chemical Engineering, Jiangxi Normal University, Nanchang, 330027, China

[*]Corresponding Authors: Shangxing Chen. Email: csxing@126.com; Ji Zhang. Email: ex1990111@163.com

Received: 15 March 2022 Accepted: 29 April 2022

ABSTRACT

(E) ω-formylcamphene was synthesized from α-pinene, the main component of turpentine, and then reacted with thiosemicarbazide to obtain (E) ω-formylcamphene thiosemicarbazide **3**, which was reacted with 14 α-bromoacetophenone compounds to obtain 14 (E) ω-formylcamphene thiazole hydrazone compounds **5a–5n**; the yields were all above 80%. The structures of the target compounds were characterized by IR, ^{1}H-NMR, ^{13}C-NMR, and HR-MS analyses. Then, 500, 250, 125, 62.5, and 31.25 mg/L drug solutions were prepared. Free radical scavenging experiments of 1, 1-diphenyl-2-picrylhydrazyl (DPPH) and 2, 2-bis (3-ethyl-benzothiazole-6-sulfonic acid) diammonium salt (ABTS) were carried out with Trolox and L-ascorbic acid as the control samples. The scavenging rates of 14 compounds for DPPH and ABTS free radicals were obtained; the IC_{50} values of scavenging free radicals were fitted using SPSS software. The results show that 14 (E) ω-formylcamphene-based thiazole hydrazone compounds exhibited good scavenging effects on the two free radicals, especially when the concentration of the drug solution was 125 and 62.5 mg/L; most compounds exceeded the scavenging efficiency of Trolox and L-ascorbic acid.

KEYWORDS

(E) ω-formylcamphene; thiosemicarbazone; thiazohydrazone; structural analysis; antioxidant activity

1 Introduction

In a biological system, oxidative stress is a state of imbalance between the oxidation and antioxidation in the body, and a negative effect produced by free radicals in the body, which is considered to be an important factor leading to aging [1,2] and disease [3,4]. A large number of reactive oxygen species (ROS) generated by oxidative stress will destroy the antioxidant defense system. Free radicals such as superoxide anion radical, hydroxyl radical, and hydrogen peroxide radical can cause oxidative damage to nucleic acids, proteins, and biofilms, leading to hypertension, diabetes, heart disease, and Alzheimer's disease [5–7]. Antioxidants can interact with free radicals to prevent the destruction of reactive oxygen species; therefore, many studies have been conducted on the design and development of new and effective antioxidants [8,9]. In recent years, the research and development of antioxidants has become an important research topic worldwide.

However, synthetic chemical antioxidants have some potential health hazards; therefore, the antioxidants prepared by the modification of natural products have attracted much attention [10–12].

Camphene, a dicyclic monoterpene compound, exists in a variety of natural volatile oils, such as camphor oil, citronella oil, turpentine oil, and cedar oil [13], and it can be prepared from the main component of turpentine α-pinene [14]. It is a renewable raw material in the fine chemical industry and can participate in many chemical reactions [15]. (E) ω-formylcamphene is synthesized by the *Vilsmeier–Haack* formylation reaction of camphene, and a series of camphene derivatives such as ω-acyl camphene, internal isocamphene alkyl methanol and alkyl ethers, alcohol acetate, and isocamphene alkyl ketone oxime can be synthesized from (E) ω-formylcamphene [16–19]. Some of these derivatives exhibit good biological activities. Thiazole is a five-atom heterocyclic compound and a very important scaffold in the pharmaceutical chemistry [20,21]. Many compounds with this structure often have antioxidant [22], antibacterial [23,24], antitumor [25], and other biological activities. The derivatives of thiazolylhydrazone compounds contain two active groups of thiazolyl ring and hydrazone (R–C=N–N–R), which may produce new compounds with higher biological activities. Therefore, they have received much attention in medicine, pesticides, and materials [26].

In this study, (E) ω-formylcamphene was prepared by the Vilsmeier-Hack formylation reaction of camphene with thiosemicarbazide to obtain (E) ω-formylcamphene thiosemicarbazide derivatives. DPPH and ABTS methods were used to determine the free radical scavenging capacity of the compounds, and the antioxidant activity of the derivatives was analyzed to provide a reference for the development of new antioxidants.

2 Experimental

2.1 Materials

All the chemicals are commercially available (Aladdin Biochemical Technology Co., Ltd., Shanghai, China). All the solvents were distilled and dried according to standard procedures. Melting points were determined using a WRS-2 melting point apparatus (Shanghai Precision & Scientific Instrument Co., Ltd., Shanghai, China). FT-IR spectra of the compounds were recorded using a Nicolet IS10 FT-IR spectrometer. Proton nuclear magnetic resonance spectra (^{1}H NMR and ^{13}C NMR) were obtained at 400 MHz using a Bruker DPX 400 spectrometer (Bruker, Germany). Spectra were recorded in $CDCl_3$ and DMSO solutions, and TMS was used as the internal standard. ESI-MS were recorded on a Hybrid Quadrupole-TOF Mass Spectrometer. Multifunctional Enzyme Marker (SpectraMax M2, Meigu Molecular Instruments Co., Ltd., Shanghai, China) was selected to measure the activities during the experiment.

2.2 Synthesis

2.2.1 Formylcamphene 2 was Synthesized by Vilsmeier–Haack Formylation Reaction

In a three-necked flask, DMF (90–100 mL) was added at low temperature and then $POCl_3$ (74 mL) was dropped through a drip funnel under stirring conditions to maintain the temperature below 10°C. After dropping, the temperature was increased to 60°C–70°C, and 105 g camphene dissolved in 1, 2-dichloroethane solution (40 mL) was slowly dropped into the bottle through the drop funnel under stirring conditions. The mixture was stirred at 80°C–85°C for additional 8 h under condensation and circumfluence conditions. At the end of the reaction, 200–300 g cold water was added and cooled to separate the organic layer. Then saturated NaOH was added to neutralize the water layer to pH 7–8. The organic layer was extracted with toluene, and washed with saturated salt water (3 ×, 100 mL). (E) ω-formylcamphene **2** was obtained by vacuum distillation.

2.2.2 Synthesis of (E) ω-Formylcamphene Thiosemicarbazone 3

In a ground Erlenmeyer flask, a solution of thiosemicarbazide (0.05 mol) was prepared in an ethanol aqueous solution (60 mL, V_{ETOH}:V_{H2O} = 1:1). The resulting solution was stirred for 15 min at 50°C until the solid was

dissolved. Then, the corresponding formylcamphene **2** (0.05 mol) was added slowly, and the mixture was stirred at 40°C–45°C for additional 24 h under condensation and circumfluence conditions. The reaction mixture was cooled and stand for 1–2 h. The reaction mixture was filtered to obtain a solid and washed with petroleum ether (3 ×, 100 mL). The crude product was recrystallized from ethanol to afford compound **3**.

2.2.3 Synthesis of (E) ω-Formylcamphene-Based Thiazole Hydrazone Derivatives 5a–5n

In a ground Erlenmeyer flask, the appropriate (E) ω-formylcamphene-based thiosemicarbazone **3** (0.05 mol) and substituted 2-bromoacetophenone **4** (0.05 mol) were added to an absolute alcohol solution (60 mL). The resulting mixture was stirred at room temperature for 5–6 h. The reaction mixture was filtered to obtain a solid. The resulting solid was washed with petroleum ether (3 ×, 100 mL), filtered, and dried under vacuum to afford (E) ω-formylcamphene-based thiazole hydrazone derivatives **5**.

The characterization data of the compounds (**3**, **5a**–**5n**) are shown in Table 1.

Table 1: Structural analysis of (E) ω-formylcamphene-based thiazole hydrazone derivatives

Compounds	Characterization data
3 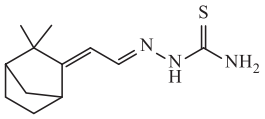	white solid, yield 86.2%, m.p. 129.7°C; IR (cm^{-1}): 3425, 3257, 3151, 3022, 1642, 1530, 1193; ^{1}H NMR ($CDCl_3$, 400 MHz) δ_H: 9.99 (s, 1H, NH), 7.85 (d, J = 9.6 Hz, 1H, $_{11}$-CH), 7.06, 6.36 (2 s, 2H, NH_2), 5.71 (d, J = 9.6 Hz, 1H, $_{10}$-CH), 3.16 (s, 1H, $_{1}$-CH), 1.97 (s, 1H, $_{4}$-CH), 1.73 (m, 2H, $_{5}$-CH_2), 1.64 (m, 1H, $_{6}$-CH), 1.44 (m, 1H, $_{6}$-CH), 1.32 (m, 1H, $_{7}$-CH), 1.19 (m, 1H, $_{7}$-CH), 1.07 (s, 3H, $_{8}$-CH_3), 1.04 (s, 3H, $_{9}$-CH_3); ^{13}C NMR ($CDCl_3$, 100 MHz) δ_C: 176.80 (S=C), 172.65(C_{-2}), 145.05 (C_{-11}), 111.95 (C_{-10}), 47.22 (C_{-1}), 43.44 (C_{-3}), 42.35 (C_{-4}), 37.37 (C_{-7}), 28.29 (C_{-8}), 28.00 (C_{-6}), 25.17 (C_{-9}), 23.50 (C_{-5}); ESI-MS *m/z*: 236.12 $[M-H]^-$, 238.17 $[M+H]^+$.
5a 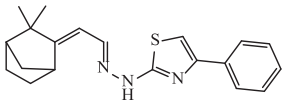	light yellow solid, yield 85.6%, m.p.152°C; IR (cm^{-1}): 3369, 3056, 1626; ^{1}H NMR ($CDCl_3$, 400 MHz) δ_H: 12.91 (br, 1H, N–H), 8.19 (d, J = 10 Hz, 1H, $_{11}$-CH), 7.70 (d, J = 7.6 Hz, 2H, $_{2'}$-CH, $_{6'}$-CH), 7.45 (m, 3H, $_{3'}$-CH, $_{4'}$-CH), 6.75 (s, 1H, $_{13}$-CH), 5.83 (d, J = 9.6 Hz, 1H, $_{10}$-CH), 3.27 (m, 1H, $_{1}$-CH), 2.00 (s, 1H, $_{4}$-CH), 1.51 (m, 3H, $_{5}$-CH_2, $_{6}$-CH), 1.48 (m, 1H, $_{6}$-CH), 1.37 (m, 1H, $_{7}$-CH), 1.21 (d, J = 21.2 Hz, 1H, $_{7}$-CH), 1.11 (s, 3H, $_{8}$-CH_3), 1.09 (s, 3H, $_{9}$-CH_3); ^{13}C NMR ($CDCl_3$, 100 MHz) δ_C: 176.05 (C_{-12}), 168.05 (C_{-2}), 151.71 (C_{-11}), 140.59 (C_{-14}), 130.39 ($C_{-4'}$), 129.55 ($C_{-2'}$, $C_{-6'}$), 127.31 ($C_{-1'}$), 125.74 ($C_{-3'}$, $C_{-5'}$), 111.47 (C_{-10}), 100.90 (C_{-13}), 47.41 (C_{-1}), 44.69 (C_{-3}), 42.72 (C_{-4}), 37.53 (C_{-7}), 28.31 (C_{-8}), 28.12 (C_{-6}), 25.26 (C_{-9}), 23.58 (C_{-5}); ESI-MS *m/z*: 336.16 $[M-H]^-$, 338.17 $[M+H]^+$.
5b 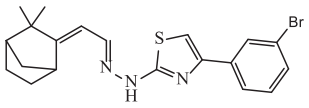	white solid, yield 86%, m.p. 156.9°C; IR (cm^{-1}): 3379, 3048, 1629, 740; ^{1}H NMR (DMSO-d6, 400 MHz) δ_H: 11.88 (br, 1H, N–H), 7.95 (m, 1H, $_{11}$-CH), 7.83 (m, 1H, $_{4'}$-CH), 7.42 (s, 1H, $_{13}$-CH), 7.38 (m, 2H, $_{6'}$-CH, $_{5'}$-CH), 5.77 (m, 1H, $_{10}$-CH, $_{13}$-CH), 3.13 (s, 1H, $_{1}$-CH), 1.95 (s, 1H, $_{4}$-CH), 1.72 (m, 3H, $_{5}$-CH_2, $_{6}$-CH), 1.43 (m, 1H, $_{6}$-CH), 1.33 (m, 1H, $_{7}$-CH), 1.14 (m, 1H, $_{7}$-CH), 1.08, 1.05 (2 s, 6H, $_{8}$-CH_3, $_{9}$-CH_3); ^{13}C NMR (DMSO-d6, 100 MHz) δ_C: 168.57 (C_{-12}), 167.90 (C_{-2}), 147.99 (C_{-14}), 144.08 (C_{-11}), 136.71 ($C_{-3'}$), 131.27 ($C_{-2'}$), 128.64 ($C_{-4'}$), 127.09 ($C_{-1'}$), 125.00 ($C_{-5'}$), 122.53($C_{-6'}$), 113.11 (C_{-10}), 105.34 (C_{-13}), 47.39 (C_{-1}), 43.36 (C_{-3}), 42.16 (C_{-4}), 37.44 (C_{-7}), 28.66 (C_{-8}), 28.27 (C_{-6}), 25.54 (C_{-9}), 23.76 (C_{-5}); ESI-MS *m/z*: 414.07 $[M-H]^-$, 416.08 $[M+H]^+$.

(Continued)

Table 1 (continued)

Compounds	Characterization data
5c 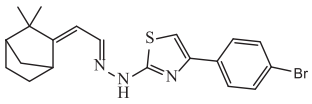	light yellow solid, yield 85.3%, m.p. 169.1°C; IR (cm^{-1}): 3362, 3046, 1618, 817, 795, 517; ^{1}H NMR (DMSO-d6, 400 MHz) δ_H: 12.32 (br, 1H, N–H), 8.05(d, J = 10 Hz, 1H, $_{11}$-CH), 7.76 (d, J = 8.4 Hz, 2H, $_{3'}$-CH, $_{5'}$-CH), 7.63 (s, 1H, $_{13}$-CH), 7.62 (d, J = 8.4 Hz, 2H, $_{2'}$-CH, $_{6'}$-CH), 5.74 (d, J = 10 Hz, 1H, $_{10}$-CH), 3.20 (s, 1H, $_{1}$-CH), 1.96 (s, 1H, $_{4}$-CH), 1.68 (m, 3H, $_{5}$-CH_2, $_{6}$-CH), 1.43 (m, 1H, $_{6}$-CH), 1.34 (m, 1H, $_{7}$-CH), 1.11 (m, 1H, $_{7}$-CH), 1.07, 1.05 (2 s, 6H, $_{8}$-CH_3, $_{9}$-CH_3); ^{13}C NMR (DMSO-d6, 100 MHz) δ_C: 169.47 (C_{-12}), 168.49 (C_{-2}), 146.90 (C_{-14}), 145.36 (C_{-11}), 132.58($C_{-4'}$), 132.07 ($C_{-3'}$,$C_{-5'}$), 130.29 (C_{-13}), 128.17 ($C_{-2'}$, $C_{-6'}$), 121.61 ($C_{-1'}$), 112.73 (C_{-10}), 47.32 (C_{-1}), 42.19 (C_{-4}), 43.39 (C_{-3}), 37.38 (C_{-7}), 28.55 (C_{-8}), 28.24 (C_{-6}), 25.45 (C_{-9}), 23.66 (C_{-5}); ESI-MS *m/z*: 414.07 $[M-H]^-$, 416.06 $[M+H]^+$.
5d 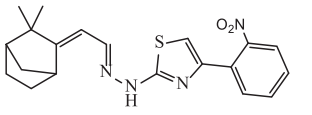	yellow solid, yield 87%, m.p. 153.2°C; IR (cm^{-1}): 3432, 3140, 1627, 1526, 1340, 759;^{1}H NMR ($CDCl_3$, 400 MHz) δ_H: 12.32 (br, 1H, N–H), 8.16 (d, J = 10 Hz, 1H, $_{11}$-CH), 8.08 (d, J = 8 Hz, 1H, $_{3'}$-CH), 7.73(m, 3H, $_{4'}$-CH, $_{5'}$-CH, $_{6'}$-CH), 6.71 (s, 1H, $_{13}$-CH), 5.83 (d, J = 10 Hz, 1H, $_{10}$-CH), 3.32 (s, 1H, $_{1}$-CH), 2.02 (s, 1H, $_{4}$-CH), 1.74 (m, 3H, $_{5}$-CH_2, $_{6}$-CH), 1.48 (m, 1H, $_{6}$-CH), 1.40 (m, 1H, $_{7}$-CH), 1.16 (m, 1H, $_{7}$-CH), 1.12, 1.09 (2 s, 6H, $_{8}$-CH_3, $_{9}$-CH_3); ^{13}C NMR ($CDCl_3$, 100 MHz) δ_C: 176.26 (C_{-12}), 167.63 (C_{-2}), 151.86 (C_{-11}), 148.10 (C_{-14}), 134.98 ($C_{-2'}$), 133.87 ($C_{-3'}$), 131.84 ($C_{-6'}$), 125.30 ($C_{-4'}$, $C_{-5'}$), 122.46 ($C_{-1'}$), 111.41 (C_{-10}), 106.30 (C_{-13}), 47.33 (C_{-1}), 43.93 (C_{-3}), 42.68 (C_{-4}), 37.60 (C_{-7}), 28.28 (C_{-8}), 28.09 (C_{-6}), 25.28 (C_{-9}), 23.56 (C_{-5}); ESI-MS *m/z*: 381.14 $[M-H]^-$, 383.15 $[M+H]^+$.
5e 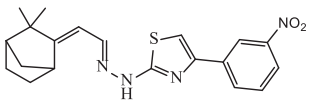	yellow solid, yield 86.3%, m.p. 172.7°C; IR (cm^{-1}): 3426, 3077, 1617, 1531, 1350, 738; ^{1}H NMR ($CDCl_3$, 400 MHz) δ_H: 12.42 (br, 1H, N–H), 8.57 (s, 1H, $_{2'}$-CH), 8.29 (d, J = 8 Hz, 1H, $_{11}$-CH), 8.20 (d, J = 8 Hz, 1H, $_{4'}$-CH), 8.15 (t, J = 9.6 Hz, 1H, $_{5'}$-CH), 7.74(d, J = 10 Hz, 1H, $_{6'}$-CH), 7.11 (s, 1H, $_{13}$-CH), 5.85(d, J = 10 Hz, 1H, $_{10}$-CH), 3.26 (m, 1H, $_{1}$-CH), 2.02(s, 1H, $_{4}$-CH), 1.75 (m, 3H, $_{5}$-CH_2, $_{6}$-CH), 1.50 (m, 1H, $_{6}$-CH), 1.39 (m, 1H, $_{6}$-CH), 1.42 (m, 1H, $_{7}$-CH), 1.20 (d, J = 20 Hz, 1H, $_{7}$-CH), 1.13 (s, 3H, $_{8}$-CH_3), 1.10 (s, 3H, $_{9}$-CH_3); ^{13}C NMR ($CDCl_3$, 100 MHz) δ_C: 176.83 (C_{-12}), 168.37 (C_{-2}), 152.13 (C_{-11}), 148.66 (C_{-14}), 138.05 ($C_{-3'}$), 131.37 ($C_{-2'}$), 131.14 ($C_{-4'}$), 128.91 ($C_{-1'}$), 124.66 ($C_{-6'}$), 120.77 ($C_{-5'}$), 111.30 (C_{-10}), 104.10 (C_{-13}), 47.36 (C_{-1}), 44.04 (C_{-3}), 42.76 (C_{-4}), 37.55 (C_{-7}), 28.28 (C_{-8}, C_{-6}), 25.26 (C_{-9}), 23.57 (C_{-5}); ESI-MS *m/z*: 383.14 $[M-H]^-$, 383.15 $[M+H]^+$.
5f 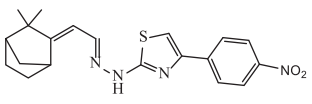	yellow solid, yield 86.7%, m.p. 188.1°C; IR (cm^{-1}): 3411, 3054, 1623, 1525, 1344, 853; ^{1}H NMR ($CDCl_3$, 400 MHz) δ_H: 11.93 (br, 1H, N–H), 8.30 (d, J = 8.4 Hz, 2H, $_{3'}$-CH, $_{5'}$-CH), 8.16 (d, J = 8.4 Hz, 2H, $_{2'}$-CH, $_{6'}$-CH), 7.98 (d, J = 9.6 Hz, 1H, $_{11}$-CH), 7.63 (s, 1H, $_{13}$-CH), 5.77 (d, J = 7.6 Hz, 1H, $_{10}$-CH), 3.14(s, 1H, $_{1}$-CH), 1.95 (s, 1H, $_{4}$-CH), 1.71 (m, 3H, $_{5}$-CH_2, $_{6}$-CH), 1.43 (m, 1H, $_{6}$-CH), 1.33 (m, 1H, $_{7}$-CH), 1.15 (m, 1H, $_{7}$-CH), 1.08 (s, 3H, $_{8}$-CH_3), 1.05 (s, 3H, $_{9}$-CH_3); ^{13}C NMR ($CDCl_3$, 100 MHz) δ_C: 168.84 (C_{-12}), 167.40 (C_{-2}), 146.91 (C_{-14}), 144.32 (C_{-11}), 140.22 ($C_{-1'}$), 129.16 ($C_{-3'}$, $C_{-5'}$), 124.05 (C_{-2}, $C_{-6'}$), 112.98 (C_{-10}), 47.41 (C_{-1}), 43.36 (C_{-3}), 42.20 (C_{-4}), 37.44 (C_{-7}), 28.65(C_{-8}), 28.24 (C_{-6}), 25.52 (C_{-9}), 23.74 (C_{-5}); ESI-MS *m/z*: 381.14 $[M-H]^-$, 383.15 $[M+H]^+$.

(Continued)

Table 1 (continued)

Compounds	Characterization data
5g 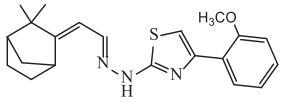	yellow solid, yield 83%, m.p. 135.8°C; IR (cm^{-1}): 3432, 3072, 1615, 1248, 1017, 781; ^1H NMR ($CDCl_3$, 400 MHz) δ_H: 13.47 (br, 1H, N–H), 8.19 (d, J = 9.6 Hz, 1H, $_{11}$-CH), 7.82 (d, J = 7.6 Hz, 1H, $_{3'}$-CH), 7.61 (t, J = 7.2 Hz, 1H, $_{4'}$-CH), 7.41 (m, 2H, $_{13}$-CH, $_{5'}$-CH), 6.93 (d, J = 6.8 Hz, 1H, $_{6'}$-CH), 5.82 (d, J = 9.6 Hz, 1H, $_{10}$-CH), 4.10 (s, 3H, OCH_3), 3.26 (m, 1H, $_1$-CH), 2.00 (s, 1H, $_4$-CH), 1.72 (m, 3H, $_5$-CH_2, $_6$-CH), 1.40–1.35 (m, 2H, $_6$-CH, $_7$-CH), 1.23 (d, J = 23.2 Hz, 1H, $_7$-CH), 1.11 (s, 3H, $_8$-CH_3), 1.08 (s, 3H, $_9$-CH_3); ^{13}C NMR ($CDCl_3$, 100 MHz) δ_C: 175.23 (C_{-12}), 167.13 (C_{-2}), 155.92 (C_{-14}), 151.16 (C_{-11}), 147.32 (C_{-13}), 137.59 ($C_{-2'}$), 134.83 ($C_{-3'}$), 131.68 ($C_{-4'}$), 128.06 ($C_{-6'}$), 121.32 ($C_{-5'}$), 115.67 ($C_{-1'}$), 111.78 (C_{-10}), 56.23 (OC), 47.35 (C_{-1}), 43.80 (C_{-3}), 42.60 (C_{-4}), 37.59 (C_{-7}), 28.33 (C_{-8}), 28.30 (C_{-6}), 25.32 (C_{-9}), 23.58 (C_{-5}); ESI-MS *m/z*: 366.17 $[M-H]^-$, 368.17 $[M+H]^+$.
5h 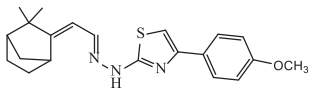	white solid, yield 82.6%, m.p. 128.5°C; IR (cm^{-1}): 3426, 3076, 1617, 1512, 1257, 1028, 831; ^1H NMR ($CDCl_3$, 400 MHz) δ_H: 12.52 (br, 1H, N–H), 8.17 (d, J = 10 Hz, 1H, $_{11}$-CH), 7.64 (d, J = 8.4 Hz, 2H, $_{3'}$-CH, $_{5'}$-CH), 6.98 (d, J = 8.4 Hz, 2H, $_{2'}$-CH, $_{6'}$-CH), 6.58 (s, 1H, $_{13}$-CH), 5.83 (d, J = 10 Hz, 1H, $_{10}$-CH), 3.84 (s, 3H, OCH_3), 3.26 (s, 1H, $_1$-CH), 2.01 (s, 1H, $_4$-CH), 1.82–1.68 (m, 3H, $_5$-CH_2, $_6$-CH), 1.48 (m, 1H, $_6$-CH), 1.39 (d, J = 10 Hz, 1H, $_7$-CH), 1.23 (m, 1H, $_7$-CH), 1.11 (s, 3H, $_8$-CH_3), 1.08 (s, 3H, $_9$-CH_3); ^{13}C NMR ($CDCl_3$, 100 MHz) δ_C: 175.88 (C_{-12}), 168.09 (C_{-2}), 161.09 (C_{-14}), 151.51 (C_{-11}), 140.41 ($C_{-1'}$), 127.28($C_{-3'}$, $C_{-5'}$), 119.91 ($C_{-4'}$), 114.88 ($C_{-2'}$, $C_{-6'}$), 111.47 (C_{-10}), 98.72 (C_{-13}), 55.48 (OC), 47.39 (C_{-1}), 43.93 (C_{-3}), 42.69 (C_{-4}), 37.53 (C_{-7}), 28.31 (C_{-8}), 28.29 (C_{-6}), 25.29 (C_{-9}), 23.60 (C_{-5}); ESI-MS *m/z*: 366.17 $[M-H]^-$, 368.18 $[M+H]^+$.
5i 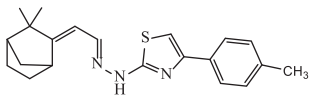	light pink solid, yield 84%, m.p. 145.1°C; IR (cm^{-1}): 3432, 3027, 1616, 1511, 818; ^1H NMR ($CDCl_3$, 400 MHz) δ_H: 13.40 (br, 1H, N–H), 8.15 (d, J = 10 Hz, 1H, $_{11}$-CH_2), 7.58 (d, J = 8 Hz, 2H, $_{2'}$-CH, $_{6'}$-CH), 7.24 (d, J = 7.6 Hz, 2H, $_{3'}$-CH, $_{5'}$-CH), 6.76 (s, 1H, $_{13}$-CH), 5.83 (d, J = 9.6 Hz, 1H, $_{10}$-CH), 3.25 (s, 1H, $_1$-CH), 2.53 (s, 3H, $_{4'}$-C–CH_3), 2.00 (s, 1H, $_4$-CH), 1.76 (m, 3H, $_5$-CH_2, $_6$-CH), 1.48 (m, 1H, $_6$-CH), 1.39 (m, 1H, $_7$-CH), 1.21 (d, J = 21.2 Hz, 1H, $_7$-CH), 1.11 (s, 3H, $_8$-CH_3), 1.08 (s, 3H, $_9$-CH_3); ^{13}C NMR ($CDCl_3$, 100 MHz) δ_C: 175.77 (C_{-12}), 168.07 (C_{-2}), 151.36(C_{-11}), 140.64 (C_{-14}), 140.38 ($C_{-1'}$), 130.20 ($C_{-2'}$,$C_{-6'}$), 125.56 ($C_{-3'}$,$C_{-5'}$), 124.44 ($C_{-4'}$), 111.46 (C_{-10}), 100.34 (C_{-13}), 47.35 (C_{-1}), 43.89 (C_{-3}), 42.66 (C_{-4}), 37.51 (C_{-7}), 28.30 (C_{-8}), 28.27 (C_{-6}), 25.27 (C_{-9}), 23.57 (C_{-5}), 21.43 (C_{-4}-CH_3); ESI-MS *m/z*: 350.17 $[M-H]^-$, 352.18 $[M+H]^+$.
5j 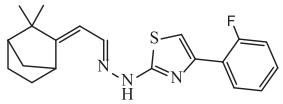	yellow green solid, yield 85%, m.p. 79.4°C; IR (cm^{-1}): 3432, 3052, 1616, 758; ^1H NMR ($CDCl_3$, 400 MHz) δ_H: 12.70 (br, 1H, N–H), 8.20 (d, J = 10 Hz, 1H, $_{11}$-CH), 7.86 (d, J = 8 Hz, 1H, $_{3'}$-CH), 7.44 (t, J = 7.2 Hz, 1H, $_{5'}$-CH), 7.31 (d, J = 7.6 Hz, 1H, $_{6'}$-CH), 7.21 (t, J = 8.8 Hz, 1H, $_{4'}$-CH), 7.06 (s, 1H, $_{13}$-CH), 5.84 (d, J = 10 Hz, 1H, $_{10}$-CH), 3.27 (s, 1H, $_1$-CH), 2.01 (s, 1H, $_4$-CH), 1.73 (m, 3H, $_5$-CH_2, $_6$-CH), 1.48 (m, 1H, $_6$-CH), 1.40 (m, 1H, $_7$-CH), 1.20 (d, J = 21.2 Hz, 1H, $_7$-CH), 1.18 (s, 3H, $_8$-CH_3), 1.09 (s, 3H, $_9$-CH_3); ^{13}C NMR ($CDCl_3$, 100 MHz) δ_C: 176.06 (C_{-12}), 167.66 (C_{-2}), 158.32 (C_{-14}), 151.76 (C_{-11}), 134.03 ($C_{-2'}$), 131.77 ($C_{-3'}$), 127.90 ($C_{-5'}$), 125.44 ($C_{-6'}$), 116.77 ($C_{-4'}$), 115.67 ($C_{-1'}$), 111.43 (C_{-10}), 105.69 (C_{-13}), 47.34 (C_{-1}), 43.91 (C_{-3}), 42.68 (C_{-4}), 37.51 (C_{-7}), 28.29 (C_{-8}), 28.26 (C_{-6}), 25.25 (C_{-9}), 23.56 (C_{-5}); ESI-MS *m/z*: 354.15 $[M-H]^-$, 356.15 $[M+H]^+$.

(Continued)

Table 1 (continued)

Compounds	Characterization data
5k 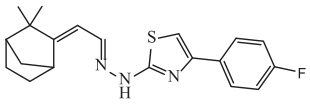	white solid, yield 85.8%, m.p. 125.2°C; IR (cm^{-1}): 3411, 3078, 1625, 1511, 838; ^1H NMR ($CDCl_3$, 400 MHz) δ_H: 12.77 (br, 1H, N–H), 8.19 (d, J = 8.4 Hz, 1H, $_{11}$-CH), 7.72 (s, 2H, $_{3'}$-CH, $_{5'}$-CH), 7.16 (s, 2H, $_{2'}$-CH, $_{6'}$-CH), 6.78 (s, 1H, $_{13}$-CH), 5.83 (d, J = 8.4 Hz, 1H, $_{10}$-CH), 3.26 (s, 1H, $_{1}$-CH), 2.02 (s, 1H, $_{4}$-CH), 1.74 (m, 3H, $_{5}$-CH_2, $_{6}$-CH), 1.45 (m, 2H, $_{6}$-CH, $_{7}$-CH), 1.18 (m, 1H, $_{7}$-CH), 1.113, 1.09 (2 s, 6H, $_{8}$-CH_3, $_{9}$-CH_3); ^{13}C NMR ($CDCl_3$, 100 MHz) δ_C: 169.24 (C_{-12}), 168.15 (C_{-2}), 162.36 (C_{-14}), 147.73 (C_{-11}), 139.40 ($C_{-4'}$), 127.86 ($C_{-3'}$, $C_{-5'}$), 127.67 (C_{-13}), 123.64 ($C_{-1'}$), 116.86 ($C_{-2'}$, $C_{-6'}$), 111.41 (C_{-10}), 47.34 (C_{-1}), 43.94 (C_{-3}), 42.70 (C_{-4}), 37.61 (C_{-7}), 28.28 (C_{-8}), 28.09 (C_{-6}), 25.26 (C_{-9}), 23.26 (C_{-5}); ESI-MS *m/z*: 354.15 $[M-H]^-$, 356.16 $[M+H]^+$.
5l 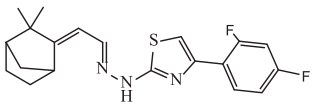	white solid, yield 86.1%, m.p. 111.5°C; IR (cm^{-1}): 3424, 3074, 1623, 1509, 845; ^1H NMR ($CDCl_3$, 400 MHz) δ_H: 12.35 (br, 1H, N–H), 8.23 (d, J = 10 Hz, 1H, $_{11}$-CH), 7.90 (m, 1H, $_{3'}$-CH), 7.06 (m, 1H, $_{5'}$-CH), 7.00 (s, 1H, $_{13}$-CH), 6.96 (d, J = 8.8 Hz, 1H, $_{6'}$-CH), 5.83 (d, J = 10 Hz, 1H, $_{10}$-CH), 3.27 (s, 1H, $_{1}$-CH), 2.01 (s, 1H, $_{4}$-CH), 1.74 (m, 3H, $_{5}$-CH_2, $_{6}$-CH), 1.49 (m, 1H, $_{6}$-CH), 1.38 (m, 1H, $_{7}$-CH), 1.21 (d, J = 20 Hz, 1H, $_{7}$-CH), 1.12 (s, 3H, $_{8}$-CH_3), 1.09 (s, 3H, $_{9}$-CH_3); ^{13}C NMR ($CDCl_3$, 100 MHz) δ_C: 176.16 (C_{-12}), 167.69 (C_{-2}), 161.35 ($C_{-4'}$), 158.81 (C_{-14}), 151.84 (C_{-11}), 133.50 ($C_{-2'}$), 129.44 ($C_{-3'}$), 112.98 ($C_{-5'}$), 112.95 ($C_{-6'}$), 112.41 ($C_{-1'}$), 111.43 (C_{-10}), 105.26 (C_{-13}), 47.37 (C_{-1}), 43.91 (C_{-3}), 42.70 (C_{-4}), 37.50 (C_{-7}), 28.26 (C_{-8},C_{-6}), 25.22 (C_{-9}), 23.55 (C_{-5}); ESI-MS *m/z*: 372.14 $[M-H]^-$, 374.15 $[M+H]^+$.
5m 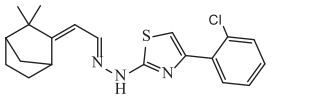	pink solid, yield 85.7%, m.p. 125.9°C; IR (cm^{-1}): 3427, 3032, 1619, 1507, 760; ^1H NMR ($CDCl_3$, 400 MHz) δ_H: 13.01 (br, 1H, N–H), 8.24 (d, J = 10 Hz, 1H, $_{11}$-CH), 7.49 (m, 1H, $_{3'}$-CH), 7.41 (m, 3H, $_{4'}$-CH, $_{5'}$-CH, $_{6'}$-CH), 7.02 (s, 1H, $_{13}$-CH), 5.84 (d, J = 10 Hz, 1H, $_{10}$-CH), 3.26 (s, 1H, $_{1}$-CH), 2.00 (s, 1H, $_{4}$-CH), 1.76 (m, 3H, $_{5}$-CH_2, $_{6}$-CH), 1.48 (m, 1H, $_{6}$-CH), 1.36 (m, 1H, $_{7}$-CH), 1.17 (m, 1H, $_{7}$-CH), 1.11, 1.08(2 s, 6H, $_{8}$-CH_3, $_{9}$-CH_3); ^{13}C NMR ($CDCl_3$, 100 MHz) δ_C: 179.70 (C_{-12}), 175.99 (C_{-2}), 167.43 (C_{-14}), 151.78 (C_{-11}), 136.56 ($C_{-2'}$), 132.21 ($C_{-1'}$), 131.36 ($C_{-3'}$), 131.09($C_{-6'}$), 130.27 ($C_{-4'}$), 127.94 ($C_{-5'}$), 111.48 (C_{-10}), 106.58(C_{-13}), 47.35 (C_{-1}), 43.89 (C_{-3}), 42.68 (C_{-4}), 37.60 (C_{-7}), 28.31 (C_{-8}), 28.10 (C_{-6}), 25.26 (C_{-9}), 23.57 (C_{-5}); ESI-MS *m/z*: 370.12 $[M-H]^-$, 372.13 $[M+H]^+$.
5n 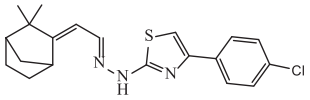	yellow solid, yield 86.2%, m.p. 130.8°C; IR (cm^{-1}): 3432, 3053, 1624, 1492, 831;^1H NMR ($CDCl_3$, 400 MHz) δ_H: 12.82 (br, 1H, N–H), 7.82 (d, J = 9.6 Hz, 1H, $_{11}$-CH), 7.67 (d, J = 8 Hz, 2H, $_{3'}$-CH, $_{5'}$-CH), 7.37 (s, 1H, $_{13}$-CH), 7.35 (m, 2H, $_{2'}$-CH, $_{6'}$-CH), 5.78 (d, J = 10 Hz, 1H, $_{10}$-CH), 2.79 (s, 1H, $_{1}$-CH), 1.95 (s, 1H, $_{4}$-CH), 1.65 (m, 3H, $_{5}$-CH_2, $_{6}$-CH), 1.42 (m, 1H, $_{6}$-CH), 1.26 (m, 1H, $_{7}$-CH), 1.20 (m, J = 24 Hz, 1H, $_{7}$-CH), 1.13 (s, 3H, $_{8}$-CH_3), 1.07 (s, 3H, $_{9}$-CH_3); ^{13}C NMR ($CDCl_3$, 100 MHz) δ_C: 171.39 (C_{-12}), 168.90 (C_{-2}), 147.95 (C_{-11}), 144.36 (C_{-14}), 135.62 ($C_{-4'}$), 135.01 ($C_{-1'}$), 129.34 ($C_{-3'}$, $C_{-5'}$), 127.10 ($C_{-2'}$, $C_{-6'}$), 111.95 (C_{-10}), 102.37 (C_{-13}), 47.43 (C_{-1}), 43.57 (C_{-3}), 42.30 (C_{-4}), 37.49 (C_{-7}), 28.42 (C_{-8}), 28.19 (C_{-6}), 25.28 (C_{-9}), 23.62 (C_{-5}); ESI-MS *m/z*: 370.12 $[M-H]^-$, 372.13 $[M+H]^+$.

Note: Abbreviations: m.p., melting point; IR, infrared; HR-MS, high-resolution mass spectrometry.

2.3 Antioxidant Studies

2.3.1 DPPH Radical Scavenging Activity

The DPPH assays of compounds **5a**–**5n** were performed using a method reported previously by Moussa et al. [27] with some modifications. $DPPH^{\bullet}$ has an intense violet color with a maximum absorbance at 517 nm, but turns colorless as unpaired electrons are scavenged by antioxidants. Ethanol was used as the solvent to dissolve compound **5**, and the final concentration was 500 μM concentration. Then, compound **5** was diluted twice to prepare five groups of concentrations. Reaction mixtures containing 50 μL of sample and 200 μL of 100 μM $DPPH^{\bullet}$ (prepared in ethanol) were incubated in a dark place at 37°C for 30 min. The absorbance was measured at 517 nm (A_1), and the percentage inhibition was calculated against a control. A blank sample containing 200 μL of ethanol in the $DPPH^{\bullet}$ solution was prepared, and its absorbance was measured (A_0). This assay uses Trolox and L-ascorbic acid as positive controls. The experiment was carried out in triplicate. The activity was determined using a microplate reader and analyzed using SPSS software to obtain IC_{50}. Radical scavenging activity was calculated using the following formula:

$$\text{inhibition}(\%) = (A_0 - A_1)/A_0 * 100\% \quad (1)$$

2.3.2 ABTS Radical Scavenging Activity

The $ABTS^{+}$ radical scavenging assays of compounds **5a**–**5n** were performed using a previously reported method by Wołosiak et al. [28] with some modifications. ABTS was dissolved in deionized water to a concentration of 7 mM. ABTS radical cation ($ABTS^{+\bullet}$) was produced by reacting ABTS solution with 1.4 mM potassium persulfate and allowing the mixture to stand in the dark at 4°C for 12–16 h before use. For the study, the $ABTS^{+\bullet}$ solution was diluted in ethanol to an absorbance of 0.70 ± 0.02 at 734 nm to form the test reagent. Ethanol was used as the solvent to dissolve compound 5, and the final concentration was 500 μM concentration. Then, compound 5 was diluted twice to prepare five groups of concentrations. Reaction mixtures containing 50 μL of sample and 200 μL of reagent were incubated at room temperature for 30 min, and the absorbance reading was taken after the initial mixing (A_1). A sample blank reading using ethanol was also taken (A_0). All the solutions were used on the day of preparation, and all determinations were carried out in triplicate. This assay used Trolox and L-ascorbic acid as positive controls. The percentage of inhibition of $ABTS^{+\bullet}$ was calculated using Eq. (1). The activity was determined using a microplate reader and analyzed using SPSS software to obtain IC_{50}.

3 Results and Discussion

3.1 Structural Characterizations

The synthetic route of (E) ω-formylcamphene-based thiazole hydrazone derivatives is shown in Fig. 1. In this experiment, (E) ω-formylcamphene **2** obtained by the *Vilsmeier–Haack* formylation reaction of camphene 1 was used as the raw material, and (E) ω-formylcamphene-based thiosemicarbazone **3** was obtained by condensation reaction. Then, the condensation of compound **3** with differently substituted 2-bromoacetophenone **4** afforded the target (E) ω-formylcamphene-based thiazole hydrazone derivatives **5a**–**5n**.

The structure of synthesized compounds (**5a**–**5n**) was determined by IR, ^{1}H NMR, ^{13}C NMR, and HR-MS analyses. IR spectrum of compound 3 showed a strong vibration absorption peak at 3425, 3257, and 3131 cm^{-1}, which can be attributed to N-H and NH_2 groups. In the IR spectra of 14 compounds **5a**–**5n**, only one absorption peak was observed in the range of 3362–3432 cm^{-1}, which is the vibrational absorption of NH bond in these compounds, and the peak for the absorption of NH_2 group completely disappeared. All the 15 compounds have C=N structure with strong absorption peaks near 1620 cm^{-1} and weak absorption peaks from 3020 cm^{-1} to 3150 cm^{-1}. They are the vibrational absorption of $_{10}$-CH, $_{11}$-CH, $_{13}$-CH, and benzene ring CH. Because a nitro (NO_2) group is present on the benzene ring of **5d**, **5e**, and **5f** molecules, two absorption peaks at 1526 and 1345 cm^{-1} appeared on the IR spectrum; **5g** and

5h showed absorption peaks at 1250 and 1020 cm^{-1}, which are the characteristic peaks of methoxy (OCH_3) group attached to a benzene ring; 13 compounds **5b**–**5n** showed a clear absorption peak in the range of 740–850 cm^{-1}, indicating the presence of one (or two) substituent(s) on the benzene ring of thiazole hydrazone compounds. In the ^1H NMR spectra, each compound showed the signals for $_{10}$-CH, $_{11}$-CH, and NH groups (5.8, 8.2, 12–13 ppm), two single-peak absorption signals for $_8$-CH_3 and $_9$-CH_3 (1.05–1.20 ppm), and proton signals of benzene ring at 6.9–8.6 ppm. The displacement values were different with different substituents on the ring. In the ^{13}C NHR spectra, different carbon atoms in each compound showed different absorption signals. In the HR-MS spectra, all compounds showed M+H and M–H values, consistent with the molecular formula.

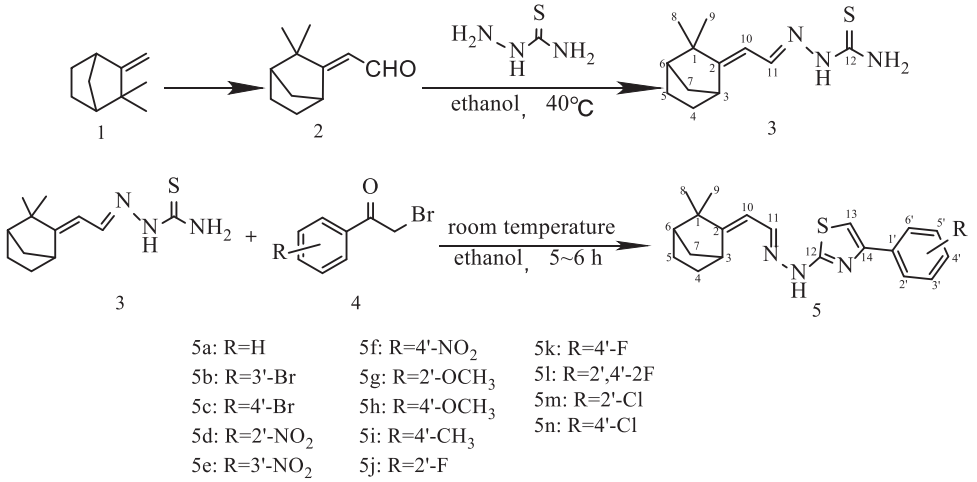

Figure 1: Synthesis of (E) ω-formylcamphene-based thiazole hydrazone derivatives

3.2 Antioxidant Activity

The scavenging rates of compounds **3**, **5a**–**5n** and the control samples Trolox and L-ascorbic acid on DPPH and ABTS free radicals at five different concentrations are shown in Tables 2 and 3.

Table 2: Determination of different concentrations of (E) ω-formylcamphene-based thiazole hydrazone derivatives for DPPH scavenging assay

Compounds	R	scavenging rate (%) at a concentration (μmol/L)				
		500	250	125	62.5	31.25
3	-	25.70 ± 1.71	11.84 ± 1.92	8.02 ± 1.11	6.83 ± 0.67	4.4 ± 0.91
5a	H	88.2 ± 0.21	88.02 ± 0.78	77.29 ± 1.22	44.14 ± 1.42	26.82 ± 1.2
5b	3-Br	91.58 ± 0.2	90.53 ± 0.9	87.8 ± 2.49	55.33 ± 2.74	37.22 ± 1.47
5c	4-Br	87.76 ± 0.88	87.27 ± 0.1	74.85 ± 0.6	39.95 ± 1.32	21.18 ± 1.69
5d	2-NO_2	93.16 ± 0.18	92.22 ± 0.94	74.42 ± 1.37	45.59 ± 4.12	25 ± 3.36
5e	3-NO_2	91.01 ± 0.82	89.77 ± 0.51	80.56 ± 0.42	45.57 ± 1.96	26.73 ± 1.39
5f	4-NO_2	91.62 ± 0.23	86.04 ± 0.23	66.14 ± 1.37	41.83 ± 0.1	23.65 ± 1.86
5g	2-OCH_3	91.46 ± 0.06	79.61 ± 0.1	59.28 ± 2.01	27.14 ± 2.84	16.14 ± 1.98
5h	4-OCH_3	85.78 ± 1.72	84.42 ± 1.63	83.74 ± 2.39	49.27 ± 2.79	27.85 ± 2.9

(Continued)

Table 2 (continued)

Compounds	R	scavenging rate (%) at a concentration (μmol/L)				
		500	250	125	62.5	31.25
5i	4-CH_3	86.01 ± 0.55	85.5 ± 0.17	85.31 ± 0.23	51.78 ± 1.77	27.51 ± 2.19
5j	2-F	92.11 ± 0.28	91.06 ± 0.25	61.33 ± 1.16	34.67 ± 0.36	21.9 ± 0.21
5k	4-F	86.14 ± 0.35	87.22 ± 0.46	73.26 ± 1.17	33.42 ± 3.28	25.31 ± 1.57
5l	2, 4–2F	89.9 ± 0.22	87.91 ± 0.76	61.1 ± 0.63	33.29 ± 2.86	18.2 ± 3.49
5m	2-Cl	91.95 ± 0.75	91.21 ± 1.04	65.09 ± 7.05	31.5 ± 7	14.12 ± 5.8
5n	4-Cl	87.69 ± 0.71	87.12 ± 0.44	78.31 ± 1.36	42.91 ± 1.18	24.89 ± 0.99
Trolox	-	97.23 ± 0.12	97.12 ± 0.19	67.22 ± 1.99	36.65 ± 3.8	19.18 ± 4.26
L-ascorbic acid	-	97.29 ± 0.36	97 ± 0.16	77.37 ± 1.04	40.06 ± 2.61	23.04 ± 1.98

Table 3: Determination of different concentrations of (E) ω-formylcamphene-based thiazole hydrazone derivatives for ABTS scavenging assay

Compounds	R	Scavenging rate (%) at a concentrations (μmol/L)				
		500	250	125	62.5	31.25
3	-	76.2 ± 1.93	59.95 ± 7.27	59.87 ± 8.83	32.67 ± 4.84	28.38 ± 5.06
5a	H	100.00	99.11 ± 0.97	83.19 ± 2.60	30.9 ± 6.74	18.18 ± 4.39
5b	3-Br	99.8 ± 0.12	99.72 ± 0.14	94.31 ± 0.66	37.21 ± 1.09	20.89 ± 2.53
5c	4-Br	99.87 ± 0.02	99.81 ± 0.09	84.99 ± 2.08	35.98 ± 1.58	18.52 ± 3.24
5d	2-NO_2	100.00	98.78 ± 0.83	64.18 ± 0.98	31.97 ± 4.56	30.19 ± 5.72
5e	3-NO_2	99.95 ± 0.06	99.63 ± 0.08	95.67 ± 2.93	59.14 ± 5.28	32.99 ± 4.57
5f	4-NO_2	99.83 ± 0.17	99.74 ± 0.28	87.75 ± 6.49	50.27 ± 8.16	29.44 ± 4.94
5g	2-OCH_3	100.00	99.83 ± 0.13	73.79 ± 9.14	27.86 ± 6.19	11.25 ± 5.08
5h	4-OCH_3	99.57 ± 0.69	98.13 ± 1.55	88.97 ± 2.47	30.15 ± 6.70	20.69 ± 0.72
5i	4-CH_3	100.00	99.63 ± 0.22	99.03 ± 0.77	43.62 ± 2.48	12.26 ± 1.52
5j	2-F	100.00	98.69 ± 1.36	68.61 ± 2.37	33.32 ± 6.86	19.96 ± 7.43
5k	4-F	99.96 ± 0.22	99.64 ± 0.1	82.42 ± 3.74	31.39 ± 3.67	15.31 ± 2.37
5l	2, 4–2F	99.85 ± 0.18	99.72 ± 0.09	72.42 ± 0.70	33.23 ± 1.33	18.54 ± 2.54
5m	2-Cl	100.00	99.95 ± 0.11	81.22 ± 3.15	40.99 ± 1.91	27.06 ± 7.68
5n	4-Cl	99.88 ± 0.09	99.81 ± 0.09	87.22 ± 4.24	41.67 ± 5.55	20.54 ± 2.30
Trolox	-	99.96 ± 0.15	98.28 ± 0.97	57.40 ± 2.96	28.31 ± 2.95	17.34 ± 1.26
L-ascorbic acid	-	99.96 ± 0.02	99.58 ± 0.19	66.19 ± 2.31	32.23 ± 1.59	14.91 ± 0.61

3.2.1 DPPH Radical Scavenging Activity

Table 2 shows that the DPPH radical scavenging rates of (E) ω-formylcamphene-based thiazole hydrazone compounds at the concentrations of 500 mg/L and 250 mg/L are slightly lower than those of the control samples, but both were above 85% (except **5g** and **5h**: 79.6% and 84.4%). When the drug

concentration decreased to 125 mg/L, the scavenging rates of **5b**, **5e**, **5 h**, and **5i** were still above 80%, higher than L-ascorbic acid (77.3%). The scavenging rates of **5a**, **5c**, **5d**, **5k**, and **5n** were also over 73%, close to L-ascorbic acid and higher than Trolox (67%). At a concentration of 62.5 mg/L, the DPPH free radical scavenging rates of eight compounds (**5a**, **5b**, **5d**, **5e**, **5f**, **5 h**, **5i**, and **5n**) were still above 40%, higher than those of L-ascorbic acid (40%) and Trolox (36.6%). These results indicate that the synthesized thiazolylhydrazone compounds exhibited good scavenging effect on DPPH free radical.

3.2.2 ABTS Radical Scavenging Activity

Table 3 shows that when the concentration of the drug solution was 500 and 250 mg/L, the scavenging rates of 14 thiazolylhydrazone compounds against ABTS free radicals were all above 98%, most of them were higher than 99.6%. Among them, the scavenging rates of **5a**, **5d**, **5 g**, **5i**, **5j**, and **5 m** at 500 mg/L were as high as 100%, better than those of the two control samples. At a concentration of 125 mg/L, the scavenging rates of **5b**, **5i**, and **5e** were still over 94%, and the scavenging rates of **5a, 5e, 5f**, **5 h**, **5k, 5 m** and **5n** were still above 80%. The scavenging rates of the remaining four compounds were higher than those of two control samples (66% and 57.4%).

According to the free radical scavenging rates listed in Tables 2 and 3, the IC_{50} values of the two free radical scavenging effects of the compounds fitted using SPSS software are shown in Table 4. The IC_{50} values of **5a**, **5b**, **5d**, **5e**, **5 h**, and **5i** were less than 65.2 μmol/L in the DPPH radical scavenging test, better than L-ascorbic acid (66.27 μmol/L). Also, **5e**, **5f**, **5k**, and **5n** were superior to Trolox (75.74 μmol/L). Among the ABTS radical scavenging activities, compounds **5e** (45.8 μmol/L) and **5f** (52.82 μmol/L) had the lowest IC_{50} values, while compounds **5b**, **5i**and **5 m** had lower IC_{50} values than 61 μmol/L. Moreover, other compounds were also better than Trolox (86.21 μmol/L) and L-ascorbic acid (79.70 μmol/L).

Table 4: Half maximal inhibitory concentration (IC_{50}) of (E) ω-formylcamphene-based thiazole hydrazone derivatives evaluated on DPPH and ABTS radicals

Compounds	R	IC_{50} (μmol/L)	
		DPPH	ABTS
3	-	>1000	114.91
5a	H	65.21	70.07
5b	3-Br	45.52	60.74
5c	4-Br	74.92	66.27
5d	2-NO_2	65.19	70.82
5e	3-NO_2	62.00	45.80
5f	4-NO_2	75.89	52.82
5g	2-OCH_3	103.56	80.36
5h	4-OCH_3	58.67	66.93
5i	4-CH_3	56.31	60.36
5j	2-F	83.11	74.84
5k	4-F	77.58	71.64
5l	2, 4–2F	90.39	73.52
5m	2-Cl	89.53	60.38
5n	4-Cl	67.63	61.54
Trolox	-	75.74	86.21
L-ascorbic acid	-	66.27	79.70

The results of antioxidant activity test show that the thiazole hydrazone derivatives that were synthesized by the blend of thiazolyl ring and hydrazone exerted better antioxidant activity on DPPH and ABTS free radical scavenging. All thiazole hydrazone derivatives have stronger antioxidant activity than (E) ω-formylcamphene thiosemicarbazone **3**. Some derivatives with different substituents exhibited moderate-to-significant antioxidant activity. For DPPH free radical, the four most potent compounds in the increasing order were **5e** < **5h** < **5i** < **5b**. For ABTS free radical, the four most potent compounds in the increasing order were **5m** < **5i** < **5f** < **5e**. This result was similar to our previous research, which demonstrated that thiazolyl ring structure and hydrazone structure are key structures for exerting antioxidant activity [29,30], and the substituted aromatic groups can capture free radicals through the degradation of potential aromatic structures [31].

4 Conclusions

In this study, 14 (E) ω-formylcamphene thiazolylhydrazone compounds were synthesized by the condensation of (E) ω-formylcamphene with thiosemicarbazide and reaction with 14 α-bromoacetophenones. The structures of all compounds were characterized by IR, ^{1}H NMR, ^{13}C NMR, and HR-MS analyses. The scavenging rates of 14 compounds against two free radicals were determined by DPPH and ABTS free radical scavenging tests, and the IC_{50} values for scavenging the two free radicals were fitted using SPSS software. The results of antioxidant activity tests show that 14 compounds had good scavenging effects on the two free radicals; especially at the concentration of 125 and 62.5 mg/L, the scavenging rate and IC_{50} values were better than the positive controls Trolox and L-ascorbic acid. In addition, the new compounds exhibited excellent antioxidant activity in vitro. At the same time, from the experimental results, it is very meaningful to synthesize (E) ω-formylcamphene thiazole hydrazone derivatives from (E) ω-formylcamphene thiosemicarbazide.

Acknowledgement: This work is supported by the National Natural Science Foundation (No. 31960295), Jiangxi Province Academic and Technical Leaders Training Program Leading Talents Project (20204BCJ22022), Special Funding for Major Scientific and Technological Research and Development in Jiangxi Province (20203ABC28W016).

Funding Statement: This research was funded by the National Natural Science Foundation (No. 31960295), Jiangxi Province Academic and Technical Leaders Training Program Leading Talents Project (20204BCJ22022), Special Funding for Major Scientific and Technological Research and Development in Jiangxi Province (20203ABC28W016).

Conflicts of Interest: The authors declare that they have no conflicts of interest to report regarding the present study

References

1. Ndlovu, G., Fouche, G., Tselanyane, M., Cordier, W., Steenkamp, V. et al. (2013). In vitro determination of the anti-aging potential of four southern african medicinal plants. *BMC Complementary and Alternative Medicine, 13,* 2–7. DOI 10.1186/1472-6882-13-304.
2. Liguori, I., Russo, G., Curcio, F., Bulli, G., Aran, L. et al. (2018). Oxidative stress, aging, and diseases. *Clinical Interventions in Aging, 2018(13),* 757–772. DOI 10.2147/cia.s158513.
3. Basu, S. (2010). Fatty acid oxidation and isoprostanes: Oxidative strain and oxidative stress. *Prostaglandins Leukot Essent Fatty Acids, 82(4–6),* 219–225. DOI 10.1016/j.plefa.2010.02.031.
4. Zhao, M. J., Yuan, S., Zi, H., Gu, J. M., Zeng, X. T. (2021). Oxidative stress links aging-associated cardiovascular diseases and prostatic diseases. *Oxidative Medicine and, Cellular Longevity, 2021,* 1–12. DOI 10.1155/2021/5896136.

5. Tan, W., Li, Q., Li, W., Dong, F., Guo, Z. Y. et al. (2016). Synthesis and antioxidant property of novel 1, 2, 3-triazole-linked starch derivatives via 'click chemistry'. *International Journal of Biological Macromolecules, 82,* 404–410. DOI 10.1016/j.ijbiomac.2015.10.007.
6. Yuan, T., Yang, T., Chen, H., Fu, D., Hu, Y. et al. (2019). New insights into oxidative stress and inflammation during diabetes mellitus-accelerated atherosclerosis. *Redox Biology, 20,* 247–260. DOI 10.1016/j.redox.2018.09.025.
7. Nascimento, V., Ferreira, N. L., Canto, R. F., Schott, K. L., Waczuk, E. P. et al. (2014). Synthesis and biological evaluation of new nitrogen-containing diselenides. *European Journal of Medicinal Chemistry, 87,* 131–139. DOI 10.1016/j.ejmech.2014.09.022.
8. Brewer, M. S. (2011). Natural antioxidants: Sources, compounds, mechanisms of action, and potential applications. *Comprehensive Reviews in Food Science and Food Safety, 10(4),* 221–247. DOI 10.1111/j.1541-4337.2011.00156.x.
9. Liu, Z. Q. (2019). Bridging free radical chemistry with drug discovery: A promising way for finding novel drugs efficiently. *European Journal of Medicinal Chemistry, 189,* 112020. DOI 10.1016/j.ejmech.2019.112020.
10. Vuong, T. V. (2021). Natural products and their derivatives with antibacterial, antioxidant and anticancer activities. *Antibiotics, 10(1),* 70. DOI 10.3390/antibiotics10010070.
11. Gonzalez-Baro, A. C., Izquierdo, D., Heras, A., Colina, A. (2020). UV/vis spectroelectrochemistry of o-vanillin: Study of the antioxidant properties. *Journal of Electroanalytical Chemistry, 859,* 113844. DOI 10.1016/j.jelechem.2020.113844.
12. Kim, M. R. (2021). Antioxidants of natural products. *Antioxidants, 10(4),* 612. DOI 10.3390/antiox10040612.
13. Cutillas, A. B., Carrasco, A., Martinez-Gutierrez, R., Tomas, V., Tudela, J. et al. (2018). Rosmarinus officinalis L. essential oils from Spain: Composition, antioxidant capacity, lipoxygenase and acetylcholinesterase inhibitory capacities, and antimicrobial activities. *Plant Biosystems, 152(6),* 1282–1292. DOI 10.1080/11263504.2018.1445129.
14. Yi, F. P., Mao, H. F. (2016). *Synthetic spice technology* (second edition). Beijing: China Light Industry Press.
15. Naoufal, E. H., Tariq, A., Naoual, E. M., Aicha, E. B., Nasreddine, E. O. et al. (2021). *In vitro* and *in vivo* biological investigations of camphene and its mechanism insights: A review. *Food Reviews International,* 1–28. DOI 10.1080/87559129.2021.1936007.
16. Xiao, Z. Q., He, Y. H. (1993). Reaction research and application in synthesis of camphenal (III): Catalytic hydrogenation. *Journal of Jiangxi Normal University (Natural Science Edition), 17(3),* 11–18.
17. Weng, Y. H., Xiao, Z. Q., Chen, J. Z., Fan, G. R., Wang, P. et al. (2015). Research progress on synthesis of camphene derivatives. *Guangzhou Chemical Industry, 43(21),* 16–21. DOI 10.3969/j.issn.1001-9677.2015.21.005.
18. Yang, L. J., Liu, H. C., Xia, D. S., Wang, S. F. (2020). Antioxidant properties of camphene-based thiosemicarbazones: Experimental and theoretical evaluation. *Molecules, 25(5),* 1192. DOI 10.3390/molecules25051192.
19. Feng, X. Z., Xiao, Z. Q., Wang, Z. D., Fan, G. R., Chen, J. Z. (2020). The synthesis and antibacterial activity of E-type camphene aldoxime and E-type camphene nitrile. *Journal of Jiangxi Normal University (Natural Science Edition), 44(2),* 4.
20. Popat, M. J., Srinivas, K., Atam, B. T., Sheshanath, V. B., Rajendra, P. P. (2021). A review on biological and medicinal significance of thiazoles. *Phosphorus, Sulfur, and Silicon and the Related Elements, 196(10),* 879–895. DOI 10.1080/10426507.2021.1945601.
21. Swarnagowri, N., Santhosh, L. G. (2019). A review on recent synthetic strategies and pharmacological importance of 1,3-thiazole derivatives. *Mini-Reviews in Medicinal Chemistry, 19(3),* 215–238. DOI 10.2174/1389557518666180816112151.
22. Md., S. S., Mohammad, M. R., Md., D. I., Abdullah, A., Junaid, U. A. et al. (2022). Synthesis, antimicrobial and antioxidant evaluation with in silico studies of new thiazole schiff base derivatives. *Journal of Molecular Structure, 1248,* 131465. DOI 10.1016/j.molstruc.2021.131465.
23. Abdel-Galil, E., Girges, M. M., Said, G. E. (2020). Synthesis and biological studies of some new thiazoles, hydrazones and azine derivatives based on 3, 5-diphenylcyclohex-2-en-1-one. *ChemistrySelect, 5(10),* 3075–3079. DOI 10.1002/slct.201904770.

24. Adole, V. A., More, R. A., Jagdale, B. S., Pawar, T. B., Chobe, S. S. (2020). Efficient synthesis, antibacterial, antifungal, antioxidant and cytotoxicity study of 2-(2-hydrazineyl) thiazole derivatives. *ChemistrySelect, 5(9),* 2778–2786. DOI 10.1002/slct.201904609.
25. Mohareb, R., Khalil, E., Mayhoub, A., Abdallah, A. (2019). Novel synthesis of pyran, thiophene, and pyridine derivatives incorporating thiazole ring and their antitumor evaluation. *Journal of Heterocyclic Chemistry, 57(3),* 1330–1343. DOI 10.1002/jhet.3870.
26. Chen, Z., Duan, W., Lin, G., Zhang, R., Luo, M. et al. (2017). Synthesis and antifungal activity of novel myrtenal-based thiazole-hydrazone compounds. *Scientia Silvae Sinicae, 53(12),* 93–101. DOI 10.11707/j.1001-7488.20171210.
27. Moussa, I., Khiari, R., Moussa, A., Mortha, G., Mhenni, M. F. (2019). Structural characterization and antioxidant activity of lignin extracted from *Ficus carica* L. *Journal of Renewable Materials, 7(4),* 345–354. DOI 10.32604/jrm.2019.04011.
28. Wołosiak, R., Drużyńska, B., Derewiaka, D., Piecyk, M., Majewska, E. et al. (2021). Verification of the conditions for determination of antioxidant activity by ABTS and DPPH assays—A practical approach. *Molecules, 27(1),* 50. DOI 10.3390/molecules27010050.
29. Shih, M. H., Ke, F. Y. (2004). Synthesis and evaluation of antioxidant activity of sydnonyl substituted thiazolidinone and thiazoline derivatives. *Bioorganic & Medicinal Chemistry, 12(17),* 4633–4643. DOI 10.1016/j.bmc.2004.06.033.
30. Shih, M. H., Su, Y. S., Wu, C. L. (2007). Synthesis of aromatic substituted hydrazino-thiazole derivatives to clarify structural characterization and antioxidant activity between 3-arylsydnonyl and aryl substituted hydrazino-thiazoles. *Chemical & Pharmaceutical Bulletin, 55(8),* 1126. DOI 10.1248/cpb.55.1126.
31. Mitra, I., Saha, A., Roy, K. (2013). Predictive chemometric modeling of DPPH free radical-scavenging activity of azole derivatives using 2D-and 3D-quantitative structure-activity relationship tools. *Future Medicinal Chemistry, 5(3),* 261–280. DOI 10.4155/FMC.12.207.